

Preparation and Electrorheological Activity of Mesoporous Rare-Earth-Doped TiO_2

Jian B. Yin and Xiao P. Zhao*

Institute of Electrorheological Technology, Department of Applied Physics, Northwestern Polytechnical University, Xi'an, 710072, People's Republic of China

Received April 15, 2002. Revised Manuscript Received August 19, 2002

A new kind of mesoporous rare-earth-doped TiO_2 particle with a well-defined crystalline framework was synthesized under a general temperature state for use as electrorheological (ER) active material. The neutral surfactant dodecylamine (DDA) was used as a template to direct the mesoporous structure. The low-angle X-ray diffraction peak showed that the mesoporous rare-earth-doped TiO_2 had an interlayer distance of about 3.4 nm and the high-angle peaks showed that the material possessed an anatase crystalline framework. ER properties of the suspension based on this material and silicone oil were measured in a dc electric field. It had been shown that the extraordinary high yield stress over 8.1 kPa could be induced when a 3 kV/mm electric field was applied. It was 20 times higher than that of pure TiO_2 ER suspension and twice as high as that of single-doped TiO_2 ER suspension as reported in our previous works. Interestingly, the shear stress of this suspension was found to continuously increase with temperature elevation in the range 10–100 °C. These improvements were attributed to the pursuit of slow polarization and suitable conduction properties of this mesoporous-doped TiO_2 suspension in terms of the measured results of dielectric and conduction properties. The present experimental result suggests that both the active internal structure and interface or surface structure of ER particles, which merit the pursuit of suitable dielectric and conduction properties, are the key to high ER activity.

Introduction

The study of mesoporous materials has provided important fundamental insight into some new-type functional materials.^{1–5} The important characteristic of mesoporous material is that it possesses surprisingly large interface or surface areas and nanosize (2–50 nm) ordered or disordered mesoporous structure.² These characters promote much experimental activity for use in photoelectronics, catalysts, semiconductors, and so on.^{2,3} Compared with these applications, the use of mesoporous materials in electrorheological (ER) fluids has found considerably less attention, even though the large interfacial polarization has been considered to merit high ER activity.^{6–8} We focus on the use of mesoporous materials in ER fluid in the present work.

ER fluids are suspensions whose viscosity or shear strength can reversibly and quickly change under an applied external electric field.^{9,10} This property has

attracted much attention from both academic and industrial communities for potential uses in various mechanical device such as clutches, valves, damping devices, and so on.^{11–13} Regarding these applications, ER properties such as high yield stress, low current density, optimal working temperature stability, and low sedimentation are especially important to ER materials.^{6,12} Much effort has been made to design and prepare high-performance ER materials in recent years.^{14–23} Even some advanced materials systems such as semiconductive polymers,^{14,18} multi-clay coating composites,^{24–26} and nanocomposites^{27–29} have been employed

* Corresponding author. Telephone (86)-29-8495950. Fax (86)-29-8491000. E-mail xphzhao@nwpu.edu.cn.

- (1) Kresge, C. T.; Leonowicz, M. E.; Roth, W. J.; Vartuli, J. C.; Beck, J. S. *Nature* **1992**, *359*, 710.
- (2) Behrens, P. *Adv. Mater.* **1993**, *5*, 127.
- (3) Corma, A. *Chem. Rev.* **1997**, *97*, 2373.
- (4) Schüth, F. *Chem. Mater.* **2001**, *13*, 3184.
- (5) Yang, P. D.; Zhao, D. Y.; Margolese, D. I.; Chmelka, B. F.; Stuky, G. D. *Nature* **1998**, *396*, 152.
- (6) Block, H.; Rattay, P. In *Progress in Electrorheology*; Havelka, K. O., Filisko, F. E., Eds.; Plenum Press: New York, 1995; p 19.
- (7) Ikazaki, F.; Kawai, A.; Uchida, K.; Kawakami, T.; Edmura, K.; Sakurai, K.; Anzai, H.; Asako, Y. *J. Phys. D: Appl. Phys.* **1998**, *31*, 336.
- (8) Hao, T.; Kawai, A.; Ikazaki, F. *Langmuir* **1998**, *14*, 1256.
- (9) Halsey, T. C. *Science* **1992**, *258*, 761.

- (10) Winslow, W. M. *J. Appl. Phys.* **1949**, *20*, 1137.
- (11) Block, H.; Kelly, J. P. *J. Phys. D: Appl. Phys.* **1988**, *21*, 1661.
- (12) Couter, S. P.; Weiss, K. D.; Carlson, J. D. *J. Intell. Mater. Syst. Struct.* **1993**, *4*, 248.
- (13) Zhao, X. P.; Tang, H. *Chinese Patent Specification* 1996, 96236145.3.
- (14) Block, H.; Kelly, J. P.; Qin, A.; Watson, T. *Langmuir* **1990**, *6*, 6.
- (15) Bloodworth, R. In *Proceedings of 4th International Conference on ER Fluids: Mechanisms, Properties, Technology and Applications*; Tao, R., Ed.; World Scientific: Singapore, 1994; p 67.
- (16) Wen, W.; Tam, W. Y.; Sheng, P. *J. Mater. Sci. Lett.* **1998**, *17*, 419.
- (17) Cho, M. S.; Choi, H. J.; To, K. *Macromol. Rapid Commun.* **1998**, *19*, 271.
- (18) Rao, T. N.; Komoda, Y.; Sakai, N. *Chem. Lett.* **1997**, *4*, 307.
- (19) Komoda, Y.; Sakai, N. *Rao, T. N. Langmuir* **1998**, *14*, 1081.
- (20) Choi, H. J.; Lee, Y. H.; Kim, C. A.; Jhon, M. S. *J. Mater. Sci. Lett.* **2000**, *19*, 533.
- (21) Park, J. H.; Lee, Y. T.; Park, O. O. *Macromol. Rapid Commun.* **2001**, *22*, 616.
- (22) Sim, I. S.; Kim, J. W.; Choi, H. J.; Kim, C. A.; Jhon, M. S. *Chem. Mater.* **2001**, *13*, 1243.
- (23) Yin, J. B.; Guan, L. T.; Zhao, X. P. *Prog. Nat. Sci.* **2002**, *3*, 867.

to secure ER active materials. Unfortunately, the experimental results were still far from the original assumption, and present ER materials are still limited in applications either for their low yield stress or for their temperature instability or sedimentation. Recently, some ER systems made of complex particle-containing polar liquids and surfactant were found to have an extraordinary high yield strength,^{30–32} but it is doubtful that these materials have optimal duration and temperature stability in practical applications.

Physically, particle polarization has been widely accepted to be responsible for the interaction force between particles that leads to the rheological change of ER fluid. Common polarization³³ and conduction models³⁴ are related to only the dielectric constant and conductivity difference between particle and continuous phase, and do not consider the effect of dynamic conditions including flow and frequency. Recently, researchers proposed the dynamic polarization mechanism and considered that the slow polarization, in particular the interfacial polarization, was mainly responsible for ER effect.^{6–8} This mechanism involved not only the polarizability (related to the high dielectric constant, ϵ) but also involved the polarization time and the stability of interaction between particles (related to the suitable high conductivity, σ , and dielectric loss, $\tan \delta$) under electric field and flow. Thus, the electrical parameters in connection with particle polarization, including ϵ , σ , and $\tan \delta$, are all accepted as basic factors dominating ER effect. It is well-known that the polarization mechanism (or dielectric and conduction properties) strongly depends on the natural structure of particle materials, such as molecular or crystal structure, microstructure, and so on. Thus, it is effective to modify the polarization properties (or dielectric and conduction properties) to increase ER activity by designing the active structure of ER materials. According to this idea, we had proposed a new way to increase ER activity of anatase TiO_2 by doping rare-earth (RE) ions and obtained high yield stress of 5.0 kPa under 3 kV/mm dc electric field.^{35–37} This stress value is 10 times higher than that of pure TiO_2 ER suspension synthesized by the same technique. The modifications of dielectric and conduction properties, which had been attributed to the activated internal structure of crystalline TiO_2 by rare-earth substitution, were verified to be responsible for the improvement of ER activity.³⁶ However, the doping mainly influenced

the internal structure, such as defects and charge carriers state, of TiO_2 . Having considered the importance of the slow polarization, in particular the interfacial polarization, designing the ER materials having a large and active interface or surface may merit the further improvement of its ER activity based on the highly active internal structure. Thereby, porous particle materials can be considered as interesting candidates to develop high performance ER materials owing to the large and active interface or surface. The typical porous ER material is pure microporous zeolite whose ER activity has been assumed to originate from active cations bound on the loose framework.^{38–40} But some of its shortcomings, such as large current density (which can strongly influence the yield stress) and instability of ER effect, limit its industrialization. Recently, siliceous mesoporous molecular sieve (MCM-41) has been proposed as an ER material.⁴¹ But the dynamic yield stress of the suspension made of 20 wt % MCM-41 in silicone oil is only 50 Pa under 3 kV/mm dc electric field and its ER effect is influenced by water content. These will strongly limit its further development as an ER material. In this study, we further develop a new kind of non-siliceous mesoporous RE-doped TiO_2 with well-defined crystalline framework on the basis of previous works^{35–37} and focus on the ER properties of the suspension made of such particles in silicone oil. The preliminary result shows this kind of material has an extraordinarily strong ER effect and different temperature effect compared with the single-doped TiO_2 reported in our previous works. In terms of the measured dielectric and conduction properties, we attribute the improvement of ER activity to the pursuit of slow polarization and suitable conduction properties of this mesoporous ER material.

Experimental Procedure

(24) Tam, W. Y.; Yi, G. H.; Wen, W.; Ma, H.; Loy, M. M. T.; Sheng, P. *Phys. Rev. Lett.* **1997**, *78*, 2987.
 (25) Knishi, M.; Nagashima, T.; Asako, Y. In *Proceedings of the 6th International Conference on ERF and MRS*; Nakano, M., Koyama, K., Eds; World Scientific: Singapore, 1998; p17.
 (26) Luo, C. R.; Tang, H.; Zhao, X. P. *Int. J. Mod. Phys. B* **2001**, *15*, 672.
 (27) Choi, H. J.; Kim, J. W.; Noh, M. H.; Lee, D. C.; Suh, M. S.; Shin, M. J.; Jhon, M. S. *J. Mater. Sci. Lett.* **1999**, *18*, 1505.
 (28) Zhao, X. P.; Lu, J. *Chinese Patent Specification* 01106797.7, 2001. Lu, J.; Zhao, X. P. *J. Mater. Res.* **2002**, *15*, 2258.
 (29) Wang, B. X.; Zhao, X. P. *J. Mater. Chem.* **2002**, *14*, 2869.
 (30) Zhang, Y. L.; Lu, K. Q.; Rao, G. H.; Tian, Y.; Zhang, S. H.; Liang, J. K. *Appl. Phys. Lett.* **2002**, *80*, 891.
 (31) Zhao, X. P.; Duan, X. J. *Colloid Interface Sci.* **2002**, *251*, 376.
 (32) Wang, B. X.; Zhao, X. P. *J. Mater. Chem.* **2002**, *12*, 1865.
 (33) Davis, L. D. *J. Appl. Phys.* **1992**, *72*, 134.
 (34) Atten, P.; Foulc, J.-N.; Felici, N. *Int. J. Mod. Phys. B* **1994**, *8*, 2731.
 (35) Zhao, X. P.; Yin, J. B.; Xiang, L. Q. *Chinese Patent Specification* 99115944.6, 1999.
 (36) Yin, J. B.; Zhao, X. P. *J. Phys. D: Appl. Phys.* **2001**, *34*, 2063.
 (37) Zhao, X. P.; Yin, J. B. *Chem. Mater.* **2002**, *14*, 2258.

(38) Filisko, F. E.; Radzilowski, L. H. *J. Rheol.* **1990**, *34*, 539.
 (39) Conrad, H.; Sprecher, A. F.; Choi, Y.; Chen, Y. *J. Rheol.* **1991**, *35*, 1393.
 (40) Böse, H. *Int. J. Mod. Phys. B* **1999**, *13*, 1878.
 (41) Choi, H. J.; Cho, M. S.; Kang, Y. K.; Ahn, W. S. *Microporous Mesoporous Mater.* **2000**, *39*, 19.
 (42) Zhao, X. P.; Yin, J. B. *Chinese Patent Specification* 02114691.8, 2002.

obtain crystallized mesoporous RE-doped TiO_2 . (Notice that the acid condition and temperature will strongly influence the crystal phase. This has been especially reported in our other paper). After centrifugal separation and washing, the sample was dried at 80 °C for 48 h in a vacuum to obtain resulting materials.

The X-ray powder diffraction (XRD) patterns of samples were carried out on an X-ray diffractometer (D/MAX-IIIC) with $Cu K\alpha$ irradiation with scan rates of 2°/min. The transmission electron microscopy (TEM) was carried out on an electron microscope (JEM-200CX). The samples for TEM were prepared by dispersing the final powders in ethanol, which was then dropped onto carbon–copper grids. Infrared spectra were recorded by employing a Fourier transform infrared spectrometer (EQUINOX55) and the KBr disk method. Thermogravimetry (TG) was carried out on a thermal analyzer (SH-500 NET2SCH, Gerateban Gabh) to estimate the adsorption ability to moisture in the mesoporous materials in the temperature range from 20 to 300 °C with a heating rate of 5 °C/min. The nitrogen adsorption isotherms and special surface areas were obtained using a Micromeritics (ASAP-2010) at -196 °C. The special surface areas were calculated using the Brunauer–Emmett–Teller (BET) equation.

Preparation of ER Suspensions. First, the produced materials were further dehydrated in a vacuum at 150 °C for 8 h to remove the adsorbed moisture. Second, the dried samples were mixed quickly with dimethyl-silicone oil ($\epsilon_f = 2.60\text{--}2.80$, $\rho_f = 0.997\text{--}1.003 \text{ g/cm}^3$, and $\eta = 500 \text{ mPa}\cdot\text{s}$ at 25 °C) in different particle concentrations to produce ER suspensions. No additives were added into the suspensions. Finally, the suspensions were specially ground for 2 h for well-mixing the particles with silicone oil.

Rheological Measurements. Rheological experiments were performed by using a coaxial cylinder rotational viscometer (NXS-11) with a Couette geometry (T3 and T4), a dc high-voltage generator (WYZ-010), and thermal instrument of oil bath (the heating range was from 0 to 150 °C, the heating rate was about 1.0–2.0 °C/min). The gaps of T3 and T4 were (2.00 ± 0.01) mm and their maximum measurable stresses were 2.760 and 11.420 kPa, respectively. The current density of viscometer was limited to 0.5 mA/cm². The maximum voltage of the dc high-voltage generator was 10 kV and the current was limited to 2.0 mA. The suspensions were placed into the gap between the stationary cup and the rotating bob. Before reading stresses, we had the suspensions initially sheared for 30 min and then applied the electric field. The static yield stress was read out from the controlled shear stress mode measurements. The ER suspension is sheared by an applied mechanical torque until the particle chain structure is broken so that slipping occurs between the cup and bob. Thereby, the shear rate is observed when the flow of the ER suspension starts. The stress at this point is known as a static yield stress.⁴³ The dynamic flow behaviors were measured in the shear rate range from 1.605 to 103.8 s⁻¹. The temperature dependence of shear stress was measured at a low shear rate of 1.605 s⁻¹. The shear stress in this low shear rate condition mainly comes from electrostatic interaction between particles rather than hydrodynamic forces. Therefore, only electrostatic interaction and thermal contribution control the temperature effect.^{44,45}

Electrical Measurements. The measuring means used in the previous works were still employed in this study.^{36,37} Because of the difficulty of directly measuring the dielectric and conduction properties of particles, we used suspensions to perform the dielectric and conduction investigation. Having considered the influence of the particles arrangement induced by an external electric field on the dielectric property,⁴⁶ we still kept the ER suspensions in a random dispersal system whose structure would not be disturbed by the bias field of 2

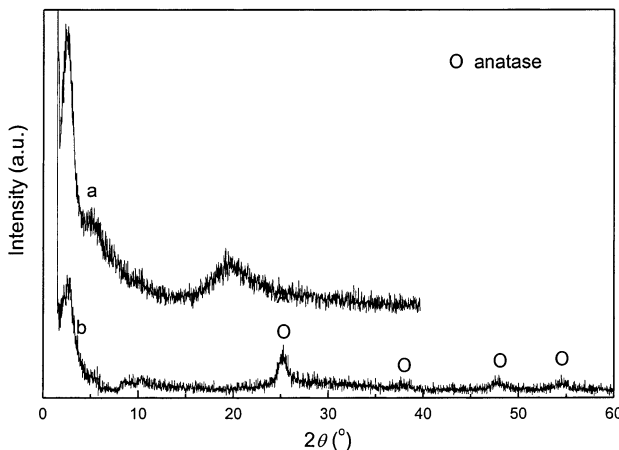


Figure 1. XRD patterns of mesoporous RE-doped TiO_2 (a) before hydrothermal and acid treatment, (b) after hydrothermal and acid treatment.

V/mm in order to make a reasonable comparison with the previous works. The capacitance C and dielectric loss tangent ($\tan \delta$) of suspensions were measured by an automatic LCR meter (WK-4225) with a temperature control instrument in the range from 0 to 120 °C at the frequency, ω , of 10², 10³, and 10⁴ Hz, respectively. The dielectric constant, ϵ , and ac conductivity, σ_{ac} , were derived from the measured C according to the conventional relations in the following, respectively:

$$\epsilon = Cd/(\epsilon_0 S) \quad (1)$$

$$\sigma_{ac} = \omega \epsilon_0 \epsilon \tan \delta \quad (2)$$

where ϵ_0 is the dielectric constant of vacuum (i.e., $8.85 \times 10^{-12} \text{ F}\cdot\text{m}^{-1}$), d is the thickness of gap between electrodes, and S is the contact area of the electrodes.

Conventional dc conductivity, σ_{dc} , of ER suspensions was derived from the measured current density, j , with a galvanometer in a high dc electric field, E_0 , of 2 kV/mm according to the following relation:

$$\sigma_{dc} = j/E_0 \quad (3)$$

Results and Discussion

Characteristics. Figure 1 shows the XRD patterns of the samples. Before hydrothermal and acid treatment, the single peak at a low 2θ angle about 2.760° indicates that the as-made sample possesses a lamellar mesoporous structure. The interlayer distance is 31.984 Å. But the crystalline peak is not found at high 2θ angle, which indicates that the channel walls of the as-made sample are made of amorphous TiO_2 . After hydrothermal and acid treatment, the diffraction peak can be still found at low 2θ angle about 2.640°, while it becomes broad and the intensity becomes weak. This indicates that the mesoporous structures still remained after hydrothermal and acid treatment but they are the less of long-range order.^{47,48} The interlayer distance is 33.438 Å. Interestingly, we have also found the clear diffraction peaks at high 2θ angle that represent the characteristic of anatase crystalline phase, which indicates that there are a lot of anatase nanocrystallites on the channel walls in mesoporous-doped TiO_2 after hydrothermal and acid

(43) Parthasarathy, M.; Klingenberg, D. *J. Mater. Sci. Eng. R* **1996**, 17, 57.

(44) Adriani, P. M.; Gast, A. P. *Phys. Fluids* **1988**, 31, 2757.

(45) Shih, Y. H.; Conrad, H. *Int. J. Mod. Phys. B* **1994**, 8, 2835.

(46) Wen, W.; Men, S. Q.; Lu, K. Q. *Phys. Rev. E* **1997**, 55, 3015.

(47) Khushalani, D.; Ozin, G. A.; Kuperman, A. *J. Mater. Chem.* **1999**, 9, 1491.

(48) Zheng, J. Y.; Pang, J. B.; Qiu, K. Y.; Wei, Y. *Microporous Mesoporous Mater.* **2001**, 40, 189.

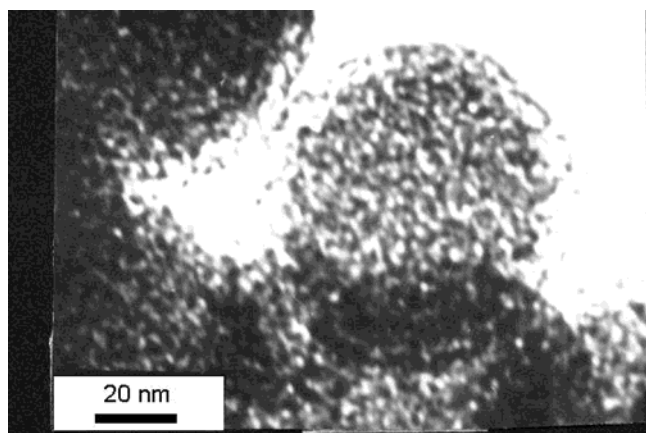


Figure 2. TEM photograph of mesoporous-doped TiO_2 after hydrothermal and acid treatment.

treatment. No peaks of the second phase at high 2θ angle are found. This indicates that the rare-earth ion substitutes for the Ti place in the synthesis process. The TEM pictures of mesoporous RE-doped TiO_2 sample show that the produced particles' diameter is basically distributed in the range of 100–1000 nm with a well-defined sphere. To well distinguish the mesoporous structure, Figure 2 shows the TEM picture of particles with a small size. It is found that the clearly mesoporous structure is apparent in a well-defined sphere particle after hydrothermal and acid-treatment. The pore size is about 2–3 nm. But it is also found that the mesophases are the less of long-range order from TEM picture, which is possibly because the crystallization of channel walls destroys the long-range ordered mesoporous structure.^{4,49}

Figure 3 shows the typical FT-IR spectra of mesoporous-doped TiO_2 . Before hydrothermal and acid treatment, the FT-IR spectra of as-made mesoporous-doped TiO_2 (Figure 3a) shows the broad bands between 3000 and 3500 cm^{-1} due to N–H stretches of DDA and O–H stretches of adsorbed water, and the sharp bands of C–H– stretching absorption bands at 2851.61 and 2922.75 cm^{-1} . The weak bands at 1383.81 and 1463.79 cm^{-1} are attributed to the C–H stretches of the CH_3 – and – CH_2 – groups in DDA. These bands provide

evidence for the incorporation of DDA into the hydrous oxide. Figure 3b shows the FT-IR spectra of mesoporous-doped TiO_2 treated by acid and drying at 150 °C for 4 h in a vacuum. A strong Ti–O– bending absorption band at about 526.77 cm^{-1} has been noted, while the C–H– stretching absorption bands at 2851.61 and 2922.75 cm^{-1} and the weak bands at 1383.81 and 1463.79 cm^{-1} due to the C–H stretches of the CH_3 – and – CH_2 – groups in DDA disappear. This indicates the template has been well-removed through acid treatment. A weak peak between 3000 and 3500 cm^{-1} may be due to O–H stretches. But the peak of free water at 1647 cm^{-1} is almost invisible. So it can be concluded that the O–H stretches may arise from a small amount of chemical adsorbed water that has formed O–H bridge with channel walls. It needs to be absolutely removed above 400 °C. However, because the increase of crystallinity at high temperature is found to destroy the mesophases, drying above 400 °C is unfitted to the presence of mesoporous structure. Furthermore, according to the FT-IR spectra, the amount of adsorbed water has become too small to influence ER effect after heat-treatment at 150 °C for 4 h in a vacuum.

Considering the strong adsorption ability of mesoporous material due to its large interface or surface areas, the dried mesoporous RE-doped TiO_2 and single RE-doped TiO_2 were used to especially investigate their adsorption ability for moisture at the temperature of 20 °C and humidity of 67%. The moisture content of mesoporous RE-doped TiO_2 determined by TG is about 4.89 wt % calculated by the weight loss around 150 °C, which is twelve times higher than that (0.37 wt %) of single RE-doped TiO_2 reported by our previous paper (Figure 4). This indicates that produced mesoporous-doped TiO_2 has a large interface or surface areas.⁵⁰ The BET surface area of mesoporous RE-doped TiO_2 is 118 m^2/g , which is significantly higher than that (9.6 m^2/g) of single-doped TiO_2 .

Electrorheological Properties. The static yield stress as a function of electric field is shown in Figure 5 for the mesoporous RE-doped TiO_2 , pure TiO_2 , and single-doped TiO_2 ER suspensions at 27% volume fraction. When a 3 kV/mm field was applied, the yield stress

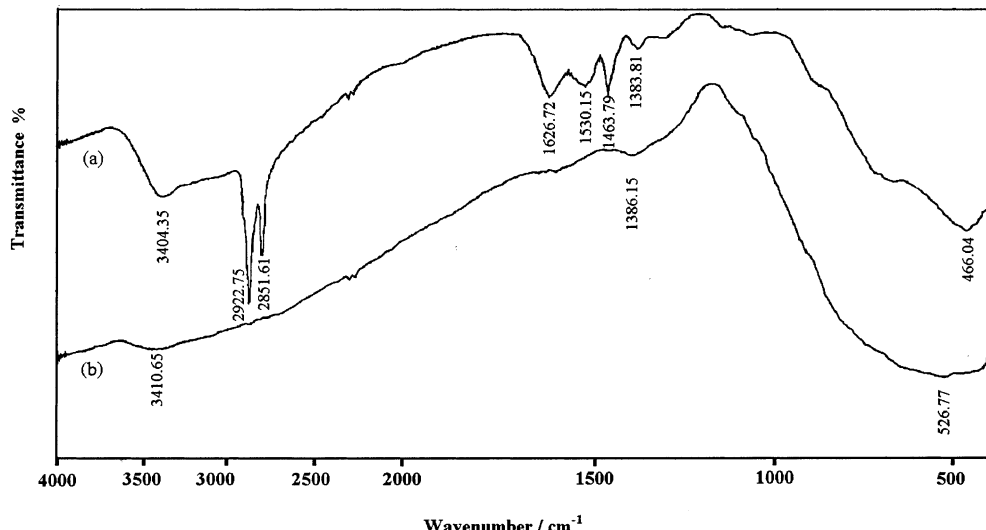


Figure 3. FT-IR spectrum of mesoporous RE-doped TiO_2 (a) before hydrothermal and acid treatment, (b) after hydrothermal and acid treatment and drying at 150 °C for 4 h.

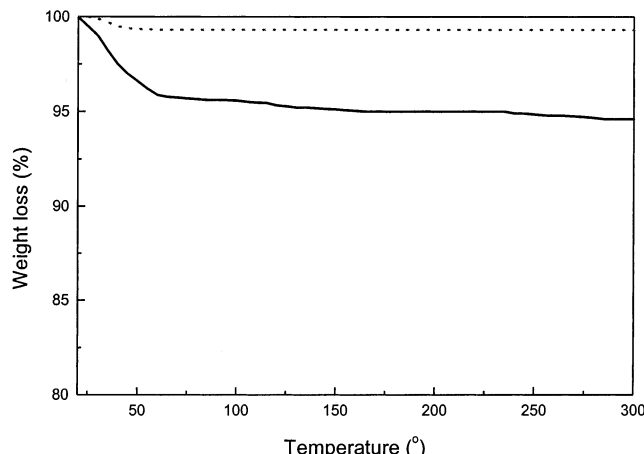


Figure 4. TG curve of mesoporous-doped TiO_2 sample (solid) and single-doped TiO_2 sample (dot) [sample, 24.228 mg; materials, mesoporous Ce-doped TiO_2 , single Ce-doped TiO_2 ; range, 20°/5.0(K/min)/300°; remark, air].

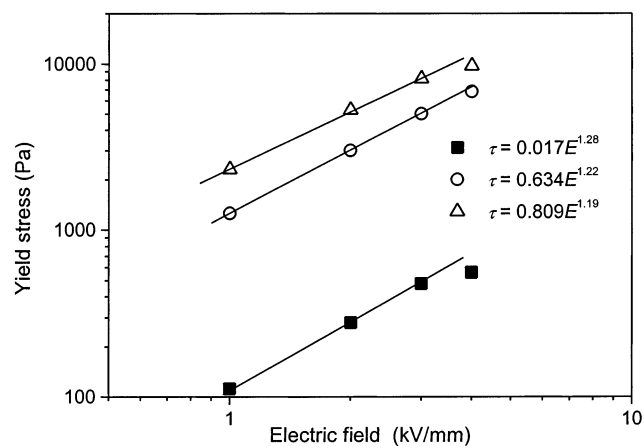


Figure 5. Static yield stress of mesoporous-doped TiO_2 ER suspension (open triangle) and ER suspensions made of single pure TiO_2 (solid square), and doped TiO_2 (open circle) as a function of electric field strength (T, 20 °C, ϕ 0.27).

of 8.1 kPa was obtained in 27% mesoporous RE-doped TiO_2 ER suspensions. However, the leaking current density was limited to no more than 8.5 $\mu A/cm^2$. The yield stress value is 20 times higher than that of pure TiO_2 ER suspension and twice as high as that of single RE-doped TiO_2 suspension at the same doping degree. Furthermore, we also synthesized the mesoporous pure TiO_2 using the same technique. Although the yield stress of suspension using such particles (about 870 Pa at 3 kV/mm) is relatively higher than that of single pure TiO_2 (about 480 Pa), it is very weak compared with that of the mesoporous-doped TiO_2 system. Therefore, the effect of rare-earth-doping is still important to ER activity, and the influence of doping degree on ER effect of mesoporous-doped TiO_2 system is almost similar to that of the single-doped TiO_2 system. We consider that the active state of the channel walls and large interface or surface areas of mesoporous structure further activate some potential factors, which had been previously verified to merit ER effect,³⁶ such as lattice distortion and defects originated from the substitution for Ti^{4+} by

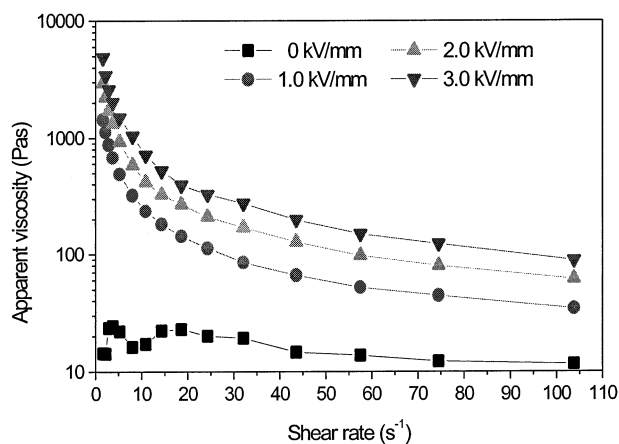
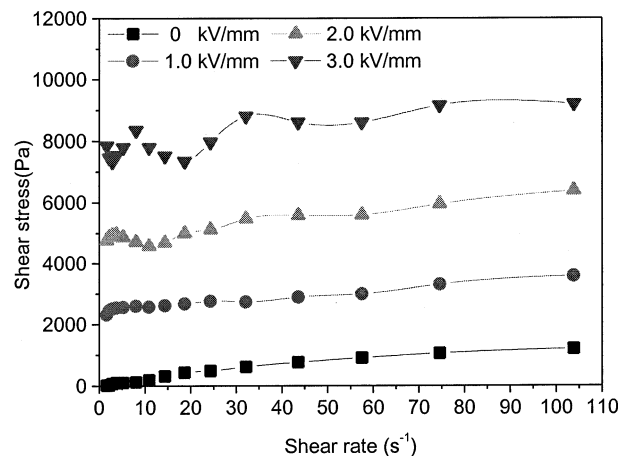


Figure 6. (a) Flow curves of shear stress of mesoporous-doped TiO_2 ER suspension as a function of shear rate (T, 20 °C; ϕ 0.27). (b) Flow curves of apparent viscosity of mesoporous-doped TiO_2 ER suspension as a function of shear rate (T, 20 °C, ϕ 0.27).

large-radius rare-earth ions. This will be discussed on the basis of the test of dielectric and conduction properties.

Figures 6(a) and (b) show the flow curve of shear stress and apparent viscosity of 27% mesoporous-doped TiO_2 suspension versus shear rate, respectively. In the absence of electric field, the suspension is not like a conventional diluted suspension that shows a Newtonian fluid behavior. The slight departure from Newtonian fluid behavior can be observed. It is not surprising to find such a non-Newtonian behavior even at zero electric fields because of the high particle concentration. In the presence of electric field, the shear stress increases quickly with electric field and the suspension possesses a significant yield stress. The large dynamic yield stress shows that the ER fluid is strongly solidified by an applied external electric field. The shear stress slightly decreases with shear rate in the low-shear-rate region smaller than 10 s^{-1} , and then increased as the shear rate was increased. This is similar to other researched results.⁵¹ According to the Mason number $Mn = (\eta_f \dot{\gamma} / 2\epsilon_0 \beta^2 E_0^2)$ (where η_f is the viscosity of oil, $\dot{\gamma}$ is the shear rate, ϵ_0 is the dielectric constant of vacuum, $\beta = (\epsilon_p - \epsilon_f / \epsilon_p + 2\epsilon_f)$, ϵ_f is the dielectric constant of oil, ϵ_p is the dielectric constant of particles, and E_0 is applied

(49) Putnam, R. L.; Nakagawa, N.; McGrath, K. M.; Yao, N.; Aksay, I. A.; Gruner, S. M.; Navrotsky, A. *Chem. Mater.* **1997**, 9, 2690.

(50) Pauly, T. R.; Pinnavaia, T. J. *Chem. Mater.* **2001**, 13, 987.

(51) Choi, H. J.; Cho, M. S.; To, K. W. *Physica A* **1998**, 254, 272.

Table 1. Dielectric Properties of the 18% ER Suspensions at 20 °C

dielectric properties	silicone oil		single- doped TiO_2 ERF ^a		mesoporous-doped TiO_2 ERF	
	ϵ	$\tan \delta$	ϵ	$\tan \delta$	ϵ	$\tan \delta$
100 Hz	2.79 ± 0.09	0.012	10.9 ± 0.5	0.180	11.8 ± 0.5	0.218
1 kHz	2.78 ± 0.04	0.009	6.55 ± 0.07	0.119	6.43 ± 0.08	0.127
10 kHz	2.78 ± 0.01	0.009	5.90 ± 0.03	0.070	5.65 ± 0.02	0.069

^a From Yin, J. B., M.S. Thesis, Northwestern Polytechnical University, China, 2001; and Yin, J. B.; Zhao, X. P. *Chin. Phys. Lett.* **2001**, 18, 1144.

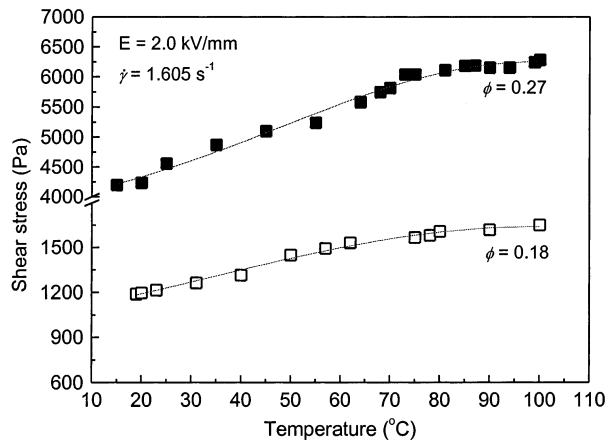


Figure 7. Temperature-dependence of mesoporous-doped TiO_2 ER suspension.

electric field),⁴³ the electrostatic interaction is more important than the hydrodynamic force in the low-shear-rate region. The slight decrease of shear stress with the increase of shear rate in the low-shear-rate region is a consequence of the destruction rate of the particle chain exceeding its reformation rate. This may also infer the influence of slow polarization on the electrostatic interaction. In the high-shear-rate region, the hydrodynamic force rather than electrostatic polarization starts to dominate the flow behavior. In addition, the flow curves at the high particle concentration of 27% are not as regular as those at the low particle concentration of 18% (figure not given here) when the high electric field over 3 kV/mm is applied. This may be due to the high zero-field viscosity or the strongly solidified structure under electric field at high particle concentration.

Interestingly, it is found that the field-induced shear stress of the mesoporous-doped TiO_2 ER suspension continuously increases with temperature in the measured temperature range from 10 to 100 °C, as shown in Figure 7, which means that the ER activity becomes stronger with increasing temperature. By comparison, the single-doped TiO_2 ER suspension was found to reach the maximum around 80 °C,³⁶ but the single and porous pure TiO_2 ER suspensions are found to decline with temperature after 45 and 50 °C, respectively. Because the temperature effect is measured at a low shear rate of 1.605 s^{-1} , the shear stress in this condition mainly comes from electrostatic interaction between particles and thermal convection.^{44,45} Therefore, the result forcefully indicates the electrostatic interaction between polarizable particles becomes stronger with temperature, even if the thermal convection becomes stronger with temperature. This will be discussed by the temperature dependence of dielectric and conduction properties.

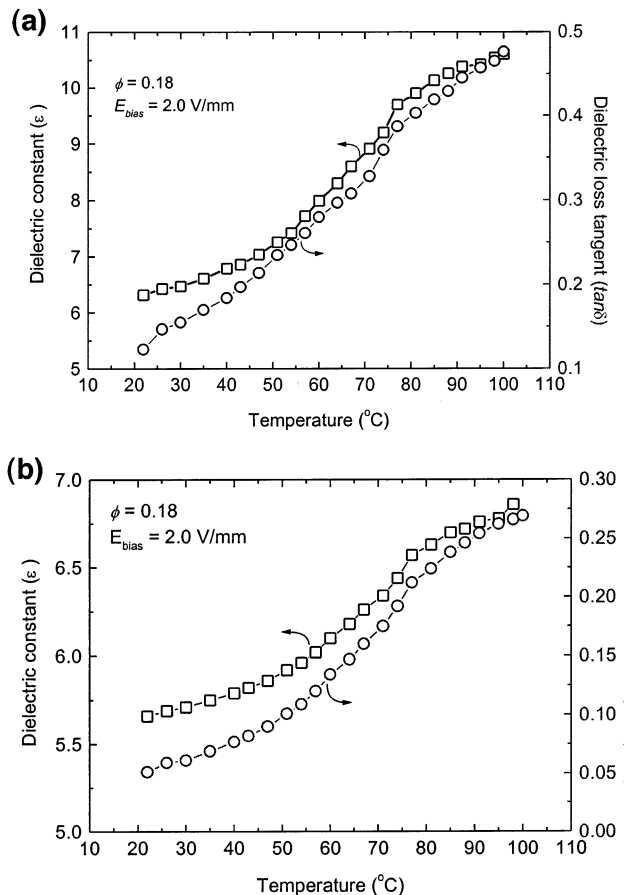


Figure 8. Temperature-dependence of dielectric constant (square) and loss tangent (circle) of mesoporous-doped TiO_2 ER suspension at frequencies of 10^3 Hz (a) and 10^4 Hz (b).

Dielectric and Conduction Properties. To clearly understand the ER activity of such material, we investigated dielectric and conduction properties of the suspension and found a significant difference between the mesoporous-doped TiO_2 and single RE-doped TiO_2 .

Table 1 lists the dielectric constant, ϵ , and loss tangent, $\tan \delta$, of the ER suspensions ($\text{Ce}/\text{Ti} = 8 \text{ mol } \%$) at room temperature. It is noted that $\tan \delta$ of mesoporous system is higher than that of single RE-doped TiO_2 ER suspensions. A large increase of ϵ as the frequency decreases ($\Delta\epsilon = \epsilon_{100} - \epsilon_{10000}$) is observed, which indicates the contribution of slow polarization, in particular interfacial polarization. Furthermore, the striking differences in temperature dependence of the dielectric constant and loss tangent are also found in the mesoporous TiO_2 comparison with the single-doped TiO_2 . Figure 8(a) and (b) show the temperature dependence of ϵ and $\tan \delta$ of the mesoporous-doped TiO_2 ER suspension at 1 kHz and 10 kHz, respectively. Obviously, the ϵ and $\tan \delta$ increase with temperature but no peaks in $\tan \delta$ are found in the temperature range

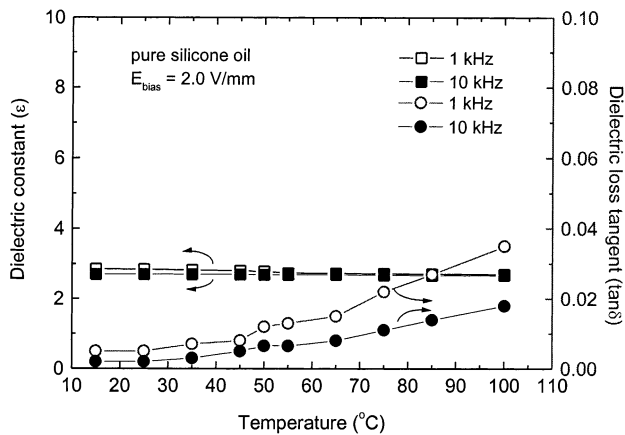


Figure 9. Temperature-dependence of dielectric properties of silicone oil used.

investigated. This is similar to the results of zeolite ER materials that also have a microporous structure,³⁹ but different from those with the single RE-doped TiO_2 .^{36,37} Because the ϵ and $\tan \delta$ of silicone oil remain independent of temperature in the range 10–100 °C (Figure 9), it is believed that the dielectric properties of ER suspensions are mainly influenced by the dielectric properties of particles dispersed in the silicone oil according to the conventional expressions of mixture approximation model: $\ln \epsilon_{mix} = \phi \ln \epsilon_p + (1 - \phi) \ln \epsilon_f$ (where ϵ_{mix} , ϵ_p , and ϵ_f are the dielectric constants of ER fluids, particles, and silicone oil, respectively; and ϕ is the particle volume fraction in ER suspension).^{52,53} Thereby, the enhancement of dielectric properties and the striking differences in temperature-dependence between mesoporous-doped TiO_2 and single-doped TiO_2 ER suspension represent the effect of mesoporous structure on the polarization of doped TiO_2 particles. The strong increase of dielectric constant at low frequency and large loss tangent, in particular the continuous elevation of dielectric constant and loss tangent with temperature, forcefully indicate that the mesoporous structure further enhances the slow polarization, especially the interfacial polarization. Practically, the dielectric properties are strongly influenced by the microstructures of particles. In the previous study,³⁶ the dielectric and conduction properties of pure TiO_2 ER suspension were found to be independent of frequency and temperature. However, the dielectric and conduction properties of single-doped TiO_2 ER suspension showed a strong dependence on frequency and temperature, and its dielectric constant tended to saturate after 85 °C and loss tangent possessed a peak around 70 °C at 10³ Hz. This had been interpreted by the basic presence of lattice distortion, defects, and impurity in TiO_2 due to RE substitution. Here, in view of the presence of defects on the channel walls, loose mesoporous structure not only increases the interface or surface areas of doped TiO_2 but also may further activate the potential factors influencing polarization and charge carriers state, such as lattice distortion, defects, and impurity that arose from RE-doping. The

(52) Sprecher, A. F.; Chen, Y.; Choi, Y.; Conrad, H. In *Proceedings of the 3rd International Conference on Electrorheological Fluids*; Tao, R., Ed; World Scientific: Singapore, 1992; p 142.

(53) Hao, T. *Appl. Phys. Lett.* **1997**, 70, 1956.

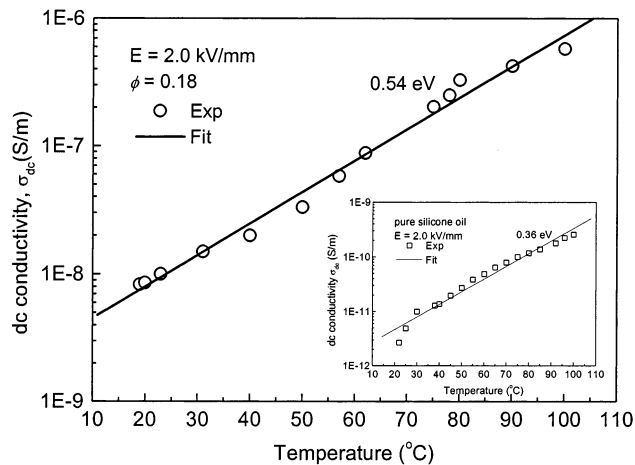


Figure 10. Temperature-dependence of dc conductivity of mesoporous-doped TiO_2 ER suspension (the temperature-dependence of dc conductivity of silicone oil used is shown in the inset).

strong increase of conductivity with temperature can also verify this discussion.

Figure 10 shows the dc conductivity σ_{dc} of mesoporous-doped TiO_2 ER suspension at 2 kV/mm with various temperature. Different from the single RE-doped TiO_2 ER suspension,³⁶ it shows a stronger temperature dependence and no saturation sign at high temperature. The conductivity is sensitive to temperature and increases by orders of magnitude with temperature. Because the dc conductivity of silicone oil is very small in the temperature range investigated, the conductivity of ER suspension is also influenced by the conductivity of particle phase mainly according to the mixture conduction approximation model of $\sigma_{mix} = \phi \sigma_p + (1 - \phi) \sigma_f$ (where σ_{mix} is the conductivity of suspension, σ_p is the conductivity of particles, σ_f is the conductivity of silicone oil, and ϕ is the particle volume fraction in suspension).⁵⁴ This indicates that the charge carriers, thermally activated in mesoporous-doped TiO_2 , are more numerous than in the single-doped TiO_2 . With the temperature increasing, more charge carriers are activated to take part in the resistive transport so that the slow polarization strength is increased. Therefore, the electric interaction becomes stronger. In addition, the result of ac conductivity, σ_{ac} , from eq 2 also gives some supported information (Figure 11). The strong elevation of σ_{ac} with temperature indicates more contribution from bound charge carriers, or polarization part. Although the adsorption of mesophases to impurity in silicone oil may influence this, the conductivity of mesoporous pure TiO_2 suspension is low (10⁻⁹ S/m at 85 °C) and insensitive to temperature. Hence, it can be concluded that the variation of conductivity is mainly originated from the microstructure of particles rather than some external factors. We consider that this is possibly because the mesoporous structure further activates the potential factors influencing charge carriers state, such as lattice distortion and defects in the TiO_2 crystal caused by large-radius RE ions substitution for Ti.

Comparing the dielectric and conduction properties with the rheological properties, we can consider that the

(54) Whittle, M.; Bullough, W. A.; Peel, D. J.; Froozian, R. *Phys. Rev. E* **1994**, 49, 5249.

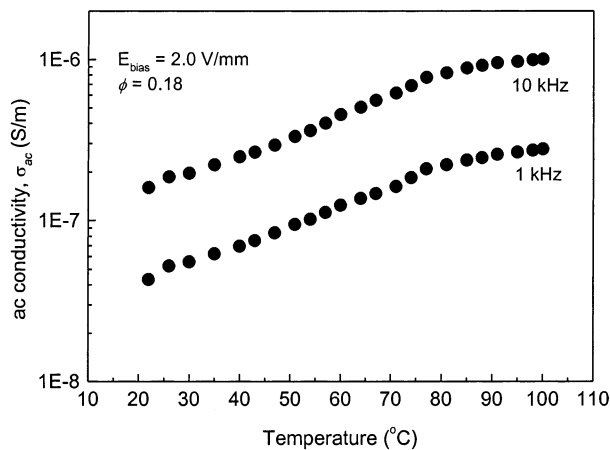


Figure 11. Temperature-dependence of ac conductivity of mesoporous-doped TiO_2 ER suspension.

further improvement of ER activity in mesoporous-doped TiO_2 is mainly attributed to the large enhancement of conductivity and slow polarization, in particular interfacial polarization. Furthermore, the elevation of its ER activity with temperature can also be attributed to the continuous improvement of slow polarization strength or the increase of dielectric and conduction properties with temperature. We suggest that the factors inducing these improvements included as follows: (1) active internal structure described in our previous work^{36,37} such as the lattice distortion, defects, and impurity within lattice structure caused by substitution for Ti with large-radius RE ions; (2) active interface or surface state, such as large interface or surface areas and loose lattice structure, caused by mesophases. Both the active internal and surface or interface structure are two indispensable conditions for high ER activity. On the other hand, why a pure crystalline TiO_2 - or BaTiO_3 -based ER system after absorption of moisture still has little ER activity even if its conductivity increases by several orders of magnitude.^{34,55} This may be mainly due to its low active natural structure. Of course, no sound theory has so far been able to give a reasonable explanation to all

observed ER phenomena. More detailed work has to be done and reported in future communications. However, our present experiment results have proposed that the active internal and interface or surface structures of ER materials, which merit pursuit of dielectric and conduction properties, will be the key to the optimal ER performance.

Conclusion

We have further developed a new kind of mesoporous RE-doped TiO_2 material on the basis of previous works. The material possessed a mesoporous structure and a well-defined anatase crystalline framework. The suspension made of this material in silicone oil showed an extraordinarily strong ER effect. Its yield stress could be up to 8.1 kPa in a 3 kV/mm dc electric field. This value was about 20 times higher than that of the pure TiO_2 and twice as high as that of the single-doped TiO_2 . Interestingly, the ER activity was found to increase with temperature elevation in the range from 10 to 100 °C. Through investigating dielectric and conduction properties, we attributed the improvement of ER activity to the increase of slow polarization and conductivity. Therefore, not only could the doping of RE for modification of the dielectric and conduction properties of TiO_2 increase the ER activity of TiO_2 , but also the presence of a mesoporous structure could further enhance its ER activity. Thereby, we further argued that the active internal and interface or surface structure, which merit the pursuit of suitable dielectric and conduction properties, were important to high ER activity in terms of our experimental facts. The combination of both factors may give a more novel and effective way to develop high-performance ER materials.

Acknowledgment. We are grateful for the help from Prof. Zhen Q. Guo on the low-angle X-ray diffraction measurement. Financial support for this research has come from the National Natural Science Foundation of China program (59832090) and the National Natural Science Foundation of China for distinguished Young Scholars program (50025207).

CM020388S

(55) Rankin, P. J.; Klingenberg, D. J. *J. Rheol.* **1998**, *42*, 639.